Applied Catalysis A: General 453 (2013) 92–101

Contents lists available at SciVerse ScienceDirect

Applied Catalysis A: General

journal homepage: www.elsevier.com/locate/apcata

Synthesis and characterization of MEL and FAU zeolites doped with transition metals for their application to the fine chemistry under microwave irradiation

Federico Azzolina Jury[a,b,c,*], Isabelle Polaert[b,1], Lionel Estel[b,1], Liliana B. Pierella[a,c]

[a] CITeQ (Centro de Investigación y Tecnología Química), Facultad Regional Córdoba, Universidad Tecnológica Nacional, 5016 Córdoba, Argentina
[b] LSPC (Laboratoire de Sécurité des Procédés Chimiques), Institut National des Sciences Appliquées INSA Rouen, France
[c] CONICET (Consejo Nacional de Investigaciones Científicas y Técnicas), Argentina

ARTICLE INFO

Article history:
Received 12 October 2012
Received in revised form
29 November 2012
Accepted 30 November 2012
Available online 14 December 2012

Keywords:
Zeolites
Dielectric properties
Microwave
Styrene oxidation

ABSTRACT

Doped zeolites with transition metals were prepared for their application to the synthesis of chemical compounds under microwave irradiation. The zeolite crystalline structures were verified by XRD. Their surface areas were determined by the BET method. Lewis and Brönsted acid sites were quantified by FTIR of adsorbed pyridine in zeolites. The characterization of acidic properties revealed the generation of new Lewis acid sites after transition metal incorporation into zeolites. The dielectric properties of compacted zeolites were measured by using a reflection method. The temperature profiles of these compacted beds were measured during heating under microwave irradiation. Heating phenomena in zeolites were interpreted using a modified Debye model. Two main dielectric mechanisms were determined in zeolites: rotational polarization phenomenon and interfacial polarization. The selective catalytic oxidation of styrene with hydrogen peroxide was studied over zeolites doped with transition metals in a batch system, under conventional and microwave heating. Benzaldehyde was the main product in all the samples under study. Styrene conversion showed an important influence of the transition metal nature and content and so, the kind of zeolite structure used. With the present experimental conditions, no difference was proved between microwave and conventional heating neither on activity nor on selectivity.

1. Introduction

Zeolites are crystalline microporous aluminosilicates of regular structure. They are composed by an anionic and rigid structure of hydrated crystalline aluminosilicates, under the configuration of three dimensional networks of infinite tetrahedrons of silicon and aluminum (primary units of construction) linked to each other, sharing vertexes and forming nonlinear oxygen bridges. Depending on the form in which the tetrahedrons are linked, different types of zeolites could be obtained. A main classification is based on the size of their pores. The pores of molecular size confer on them adsorption, catalytic and ionic exchange properties for application in the chemical industry and in the study of new applications related to intensified processes [1], "green" chemistry [2], medicine [3], optical and electrical applications [4] and nanotechnology [5].

The zeolite doped with transition metals, provides interesting catalytic properties [6]. The structure of the zeolite is very important since it determines the specific surface of the catalyst as well as the quantity of ions that could be incorporated in the zeolite framework.

On the other hand, it is interesting to study catalytic reactions under microwave irradiation. On an industrial scale, this type of heating is used especially in desorption processes [7]. The microwaves are electromagnetic waves which frequency ranges from 300 MHz to 30 GHz. The microwave irradiation allows a rapid, volumetric and homogeneous heating of dielectric materials [8–11], against the slow conventional heating governed mainly by the conduction and convection phenomena. The ability of a material to be heated under microwave irradiation is conditioned by its dielectric properties. In order to predict the response of materials to the electromagnetic waves, the knowledge of their dielectric properties is required (ε' [F m^{-1}]: dielectric constant; ε'' [F m^{-1}]: dielectric loss factor; $\tan\delta = \varepsilon''/\varepsilon'$: dissipation factor). The dielectric constant ε' is related to the electric field distribution in the material, while the dielectric loss factor ε'' is linked to the conversion of

* Corresponding author at: CITeQ (Centro de Investigación y Tecnología Química), Facultad Regional Córdoba, Universidad Tecnológica Nacional, 5016 Córdoba, Argentina. Tel.: +54 351 4690585/+33 0 232 956 654; fax: +54 351 4690585/+33 0 232 956 652.
E-mail addresses: fazzolina@scdt.frc.utn.edu.ar, federico.azzolina_jury@insa-rouen.fr (F. Azzolina Jury).
[1] Tél.: +33 0 232 956 654; fax: +33 0 232 956 652.

0926-860X/$ – see front matter © 2012 Elsevier B.V. All rights reserved.
http://dx.doi.org/10.1016/j.apcata.2012.11.046

electromagnetic energy into heat. The generation of dielectric dipoles in materials, thanks to the application of an external electric field, is due to different phenomena: dipole orientation, polarization of distortion (electronic and ionic polarization) and ionic conduction due to the mobility of free ions in the materials.

In zeolites, the responsible phenomena for dielectric heating under microwaves are mainly due to the phenomenon of dipolar orientation of the adsorbed water molecules and to the ionic conduction thanks to the mobility of ions in the channels of the cavities of the zeolites structures. The above mentioned mobility gets favored with the increase of the water content in the zeolites cavities [12].

It is interesting to study the heterogeneous catalysis with zeolites, which possess shape selectivity due to the molecular size of their pores, simultaneously to the selective dielectric heating under microwave irradiation [13]. For such purpose, the reaction of styrene partial oxidation toward benzaldehyde was chosen.

The benzaldehyde is an important product in the pharmaceutical industries, perfumery, dyes and agrochemistry, as organic intermediate [14]. Traditionally, it is obtained by homogeneous catalysis generating a significant quantity of pollutants. In addition, it is produced with impurity traces. In order to protect the environment and to apply to the "green" processes, the use of heterogeneous catalysis is necessary. For that purpose, the hydrogen peroxide was used as oxidizer agent, because it possesses high active oxide content and it only generates water as secondary product. In addition, acetonitrile was employed as solvent, thanks to its high polarity, which favors the increase of the reactant concentration in the surrounding areas of the catalyst active sites thanks to the hydrophilic character of the zeolites. On the other hand, this solvent presents a high dielectric constant that allows a good behavior under microwave.

In the present work, different sorts of zeolites (MEL and FAU) doped with transition metals were synthesized and characterized in terms of physicochemical properties and the advantages and disadvantages of each structure with regard to each cation were examined. Their crystalline structure after the ionic exchange was verified by XRD. In addition, the complex dielectric permittivities of these zeolites were determined and related to their heating capacity under microwave irradiation, by measuring the evolution of the temperature in compacted beds of zeolites during microwave heating. From a modified Debye model, the main responsible phenomena for zeolite dielectric heating and their relaxation frequencies were estimated for each zeolite with different levels of hydration. These parameters were determined and optimized by using the least-squares fitting present in Matlab® Curve Fitting Toolbox.

Styrene oxidation reaction under conventional and microwave heating was carried out. The selectivity toward benzaldehyde and the styrene conversion were compared for both heating systems. The catalysts surface area was measured by BET and the acid sites (Lewis and Brönsted) were quantified by FTIR of adsorbed pyridine in zeolites. The transition metal content in zeolites was determined by ICP.

2. Experimental

2.1. Catalyst preparation

Two different types of zeolites were used. The zeolite ZSM-11 (MEL) which offers an average pore diameter between 5 and 6 Å, with a Si/Al ratio of 17, and the zeolite Y (FAU), with larger pores (between 6 and 9 Å), with a Si/Al ratio of 2.5.

The ZSM-11 zeolite was obtained by hydrothermal synthesis using silicon dioxide as silicon source and sodium aluminate as aluminum source. The tetrabutylammonium hydroxide (TBAOH) was used as director agent. The synthesis was carried out in a Teflon reactor at 150 °C for 10 days. The obtained gel was filtered and washed exhaustively with distilled water, in order to remove the directing agent. Then, it was dried at 120 °C during 10 h. Finally, the directing agent was completely eliminated from the zeolite structure by decomposition under nitrogen flow at 500 °C during 10 h and later calcination in a muffle at the same temperature during 12 h. After all this process, the Na-ZSM-11 zeolite form was obtained. In order to facilitate the incorporation of the transition metals in the zeolite structure, it is necessary to replace the sodium ion by the ammonium ion because it is easier exchangeable. To obtain the ammonium form (NH_4-ZSM-11) an ionic exchange process was realized from the sodium form, by using an ammonium chloride solution (1 M) at 80 °C during 40 h.

On the other hand, the NH_4-Y zeolite was acquired to Sigma–Aldrich (Si/Al = 2.5).

The transition metals incorporation into zeolites structure was carried out by ionic exchange of the NH_4-zeolites with water solution containing the salt of the metallic cation at concentration of 0.05 M. Chloride salts (Cl^-) were used for Co, Ni, Fe, Cr zeolites and nitrate salts (NO_3^-) for Zn and Mn zeolites. The incorporated cations in zeolite cavities were: Co, Zn, Ni, Cr, Fe and Mn. Several zeolites were prepared with different transition metal content by varying the ion exchange time from 20 h to 60 h.

Finally, the samples were treated by desorption under atmosphere of N_2 (25 mL/min) from room temperature to 500 °C with a warming slope of 10 °C/min during 10 h and then, they were calcined at 500 °C during 12 h.

2.2. Catalyst characterization

2.2.1. Quantification of transition metal content incorporated into zeolites

The transition metal content incorporated in the zeolite structure was determined by ICP in a spectrometer Thermo Scientifics' ICP of the series iCAP 6000, using the technology proposed in Shetti et al. [15].

2.2.2. Verification of crystalline structure of zeolite catalysts

The verification of the crystalline structure was determined by X-ray diffraction technique (XRD) of the zeolite powders in a diffractometer Philips PW 3020 using radiation CuKα of wave length 0.15418 nm. The diffraction data for the MEL zeolites were collected between $2\theta = 5–60°$ and for the FAU zeolites between $2\theta = 5–50°$, in intervals of 0.1° and speed of 2° per min.

2.2.3. Determination of zeolites surface area

The zeolites surface area values were measured by using the BET method by using the single-point surface area method in an equipment ASAP 2000. Before surface area measurements, zeolites were heated at 390 °C during 50 min under inert atmosphere (70% N_2, 30% He).

2.2.4. Quantification of Lewis and Brönsted acid sites in zeolites

The adsorption of pyridine (Py) was used to quantify the Lewis and Brönsted acid sites in zeolites. It is a basic molecule, which adsorbs in a differential way on both types of acid sites, forming species which are detectable by infrared spectroscopy. The pyridine interacts with Brönsted acid sites forming the (PyH^+) species whereas the interaction of Lewis acid sites with pyridine originates the electron-donor–acceptor (EDA) adduct of Pyridine-Lewis species.

The FAU and MEL zeolites infrared measurements were carried out in a spectrometer JASCO 5300 FT/IR. The samples were compacted, forming auto supported tablets (½ in. of diameter) of pure

material (8–10 mg/cm^2). The experiments were carried out using a thermostated cell with CaF_2 windows connected to a vacuum line. The spectrum sweep was performed from 4600 cm^{-1} to 400 cm^{-1} in 16 consecutive records with a resolution of 4 cm^{-1} for each one. The wafers were heated at 400 °C in vacuum (10^{-4} Torr) for 6 h. Afterwards, in order to determine the concentration of Lewis and Brönsted acidic sites (1700–1400 cm^{-1}), pyridine (Py) (3 Torr) was adsorbed at room temperature for 12 h and desorbed for an hour at 250, 350 and 400 °C at 10^{-4} Torr.

2.3. Measurements of zeolites dielectric properties

The complex dielectric permittivities of the porous solids were measured by a reflection method coupled to a vector network analyzer (VNA) Agilent 2-PortPNA-L of the series 5230 A connected to a coaxial probe of high temperature. The measurements were carried out in an interval of frequencies between 0.5 and 20 GHz. The dielectric characterization was performed at room temperature and at different hydration levels.

The porous solids were compacted in a cylindrical container of 20 mm of height and 20 mm of diameter. In order to obtain dielectric measurements of zeolites at different water content, they were dried in an oven at 250 °C during 12 h. Then, they were placed in a desiccator under flow of N_2, to avoid the adsorption of the water molecules from air, and to cool them slowly up to room temperature. The compactions and dielectric measurements were effected in a closed container, under atmosphere of nitrogen, at room temperature (17 ± 2 °C). After every measurement, a small sample of the compacted solid was taken, to determine its water content by thermo gravimetric analysis (TGA). The TGA was carried out with the SDT equipment provided by TGA Q600 instrument, with a warming ramp of 20 °C/min from room temperature to 450 °C, under flow of nitrogen of 50 mL/min. The rest of the compacted material was placed in a great container opened in the air, in order to re-hydrate the zeolites. The processes of compaction, measurement, determination of water content and rehydration were repeated from time to time till reaching the maximum hydration level of each catalyst, the value of which depends on the zeolite structure. All measurements were carried out three times for each zeolite.

2.4. Zeolite heating under microwave irradiation

The heating of doped zeolites under microwave irradiation was carried out in an experimental apparatus described by Polaert et al. [16]. The microwave system consists of a magnetron of frequency 2450 MHz and of a wave guide WR340 which allows a monomodal propagation $TE_{1.0}$. Only zeolites with low water content were tested, in order to limit the water effect on the dielectric heating and to really evaluate the influence of the transition metals and zeolites structure.

The zeolite powders were compacted under nitrogen atmosphere inside a glass reactor of internal diameter 1.6 cm, 1 mm of wall thickness and 21 cm of height. The height of the catalyst bed was 2.8 cm. An incident power of 7–8 W was applied and the absorbed power and maximum temperatures were measured in the center of the bed, where the electrical field is maximal.

2.5. Catalytic activity measurements

In the catalytic styrene oxidation (99.5%, Alpha Aesar), hydrogen peroxide was used (30%, w/w, Alpha Aesar) as oxidizing agent and acetonitrile (analytical degree, +99.9%, Aldrich) as solvent. The reaction was carried out, under microwave irradiation and conventional heating, in a pirex glass cylindrical reactor of 23 cm of height and 4 cm of internal diameter, under mechanical agitation of 300 rpm. The above mentioned reactor presents two lateral orifices. One of them is used for the sampling at different times of the reaction. The other extremity connects the reactor to a condenser.

The reactor also possesses a third small orifice for the temperature probe introduction. For both heating systems, a molar styrene/H_2O_2 ratio of 0.9 was used; 0.4 g of catalyst and 24 mL of solvent. The molar styrene/H_2O_2 ratio of 0.9 was chosen in order to have a 10% of hydrogen peroxide excess, favoring a more complete styrene oxidation. The reaction temperature was 60 °C for all the cases [6]. The organic products were analyzed and quantified by gas chromatography using a chromatograph Varian 3400 connected to an Auto sampler 8200 of Varian Star technology, equipped with a FID detector and capillary column HP-5 5% phenyl methyl silicone (30 m × 0.32 mm di). The reaction under microwave irradiation was realized in the same waveguide WR340. For the conventional heating, the reactor was located in a silicon thermostated bath. All the reactions were carried out two times in order to verify the repeatability of the results, and each gas chromatography analysis was repeated four times for every reaction sample.

Table 1
Transition metal content for MEL zeolites.

Zeolite	ZSM-11							
Cation	Co(a)	Co(b)	Co(c)	Fe	Ni	Mn(a)	Mn(b)	H
Si/Al	17	17	17	17	17	17	17	17
Cation (wt%)	0.86	2.28	1.87	3.78	0.10	0.29	2.26	–
Cations/u.c.	0.86	2.31	1.89	4.11	0.10	0.29	2.46	–

3. Results and discussion

3.1. Characterization of MEL and FAU zeolites

The results of XRD characterization indicate that the MEL zeolites did not lose their crystalline initial structure, after all the chemical and thermal treatments. On the other hand, the stability of the FAU zeolites, during the ionic exchange process with transition cations, depended on the acidity of the saline solution used. The zeolite Cr–H–Y totally lost its crystalline structure and Fe–H–Y lost it in a partial way. For that reason, they were both rejected from the present study. This is partly due to the instability of zeolites Y at low Si/Al ratios [17]. The XRD patterns of exchanged zeolites are shown in Fig. 1. The surface area of MEL zeolites was 350 m^2/g whereas the value for the FAU zeolites was 600 m^2/g approximately. It is necessary to emphasize that the surface area of the zeolites did not significantly changed after the thermal treatments and ionic exchange processes.

The mass transition metal content for each zeolite (wt%) was measured by ICP. From these values, the number of transition cations for each unit cell of zeolites structures was calculated. The transition metal content for each zeolite is detailed in Tables 1 and 2. For the MEL structure this value goes from 0.1 to 0.9 cations per unit cell located principally in the alpha and beta sites in agreement with Dedecek et al. [18], whereas for the FAU structure, this quantity is between 5 and 10 cations per unit cell, located in the sites I (hexagonal prism) and the II (supercavity), according to Frising and Leflaive [19]. The number of transition cation

Table 2
Transition metal content for FAU zeolites.

Zeolite	Y			
Cation	H	Zn	Co(a)	Co(b)
Si/Al	2.5	2.5	2.5	2.5
Cation (wt%)	–	7.08	5.13	3.94
Cations/u.c.	–	14.51	11.43	8.66

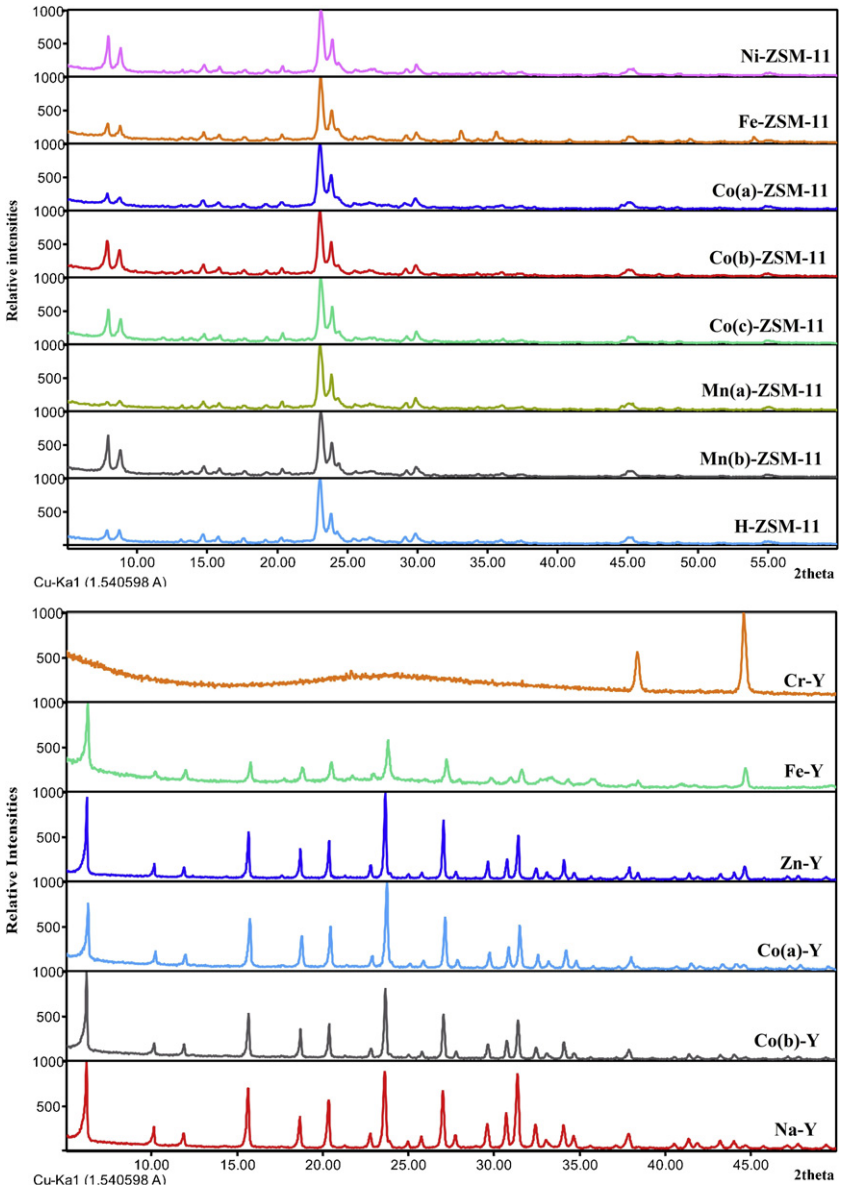

Fig. 1. XRD patterns of exchanged MEL and FAU zeolites.

in the zeolites unit cells was calculated from the transition content metal determined by ICP, by considering that the transition metal was totally under the ionic form. In case of the existence of transition metal oxides, the estimated values would represent the maximum number of transition metal cations in the zeolites unit cells.

The dielectric properties measured on FAU and MEL zeolites depend strongly on the water content. These results agree with those obtained in a previous work for different zeolites FAU and LTA [12]. These two types of zeolites possess a very different water adsorption capacity (7 wt%-dry for ZSM-11 against 30 wt%-dry for Y) due to the different Si/Al ratio and the kind of structure. The FAU zeolites present higher values of complex dielectric permittivities than the MEL ones, for all the water content range. The dielectric properties values increase in a classic way with the water content for all the zeolites. When the zeolites are hydrated, the water molecules coordinate the transition cations reducing their interaction with the negative framework of the zeolite, facilitating their mobility across the structure. Thus, the phenomenon of ionic conductivity becomes more significant.

For a given water content, the comparison of the dielectric properties of the different doped solids shows a clear influence of the transition metal cation. Hydrated or not, the zeolites MEL see their dielectric properties increasing in the sense: Co(c) < Co(b) < Co(a) < Mn(b) < Mn(a) < Ni < Fe < H due to the diminution of the transition metal content in the zeolite framework. This trend is presented in Fig. 2.

Tables 1 and 2 indicate that the transition metal content trend is: Co(c) (1.87%) < Co(b) (2.28%) < Co(a) (0.86%) < Mn(b) (2.26%) < Mn(a) (0.29%) < Ni (0.10%) < Fe (3.78%) < H (0%). The influence of the nature of the transition metal and its content in zeolites framework could be discussed. In first place, the trend with regard to the transition metal nature is: Co < Mn < Ni < Fe < H. This first trend shows that the incorporation of transition metal into zeolites decrease the dielectric properties values since the H-zeolite dielectric properties values are greater than doped zeolites. In second place, the transition metal content for each zeolite could be evaluated. For Co and Mn zeolites, it was found that the augmentation of transition metal content decrease their dielectric properties values, with the exception of Co(c) and Co(b), due to their dielectric properties

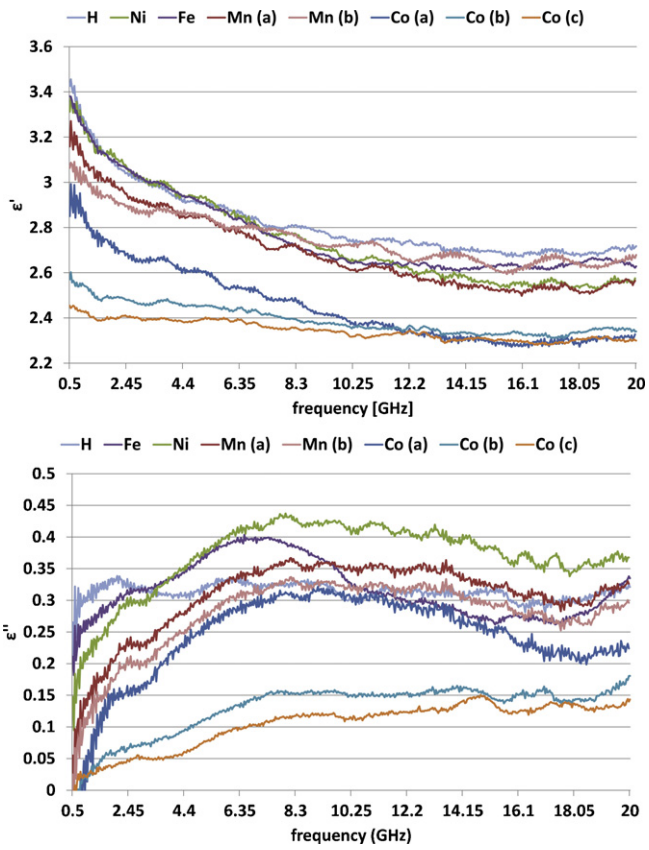

Fig. 2. Permittivity values (ε' and ε'') for MEL zeolites.

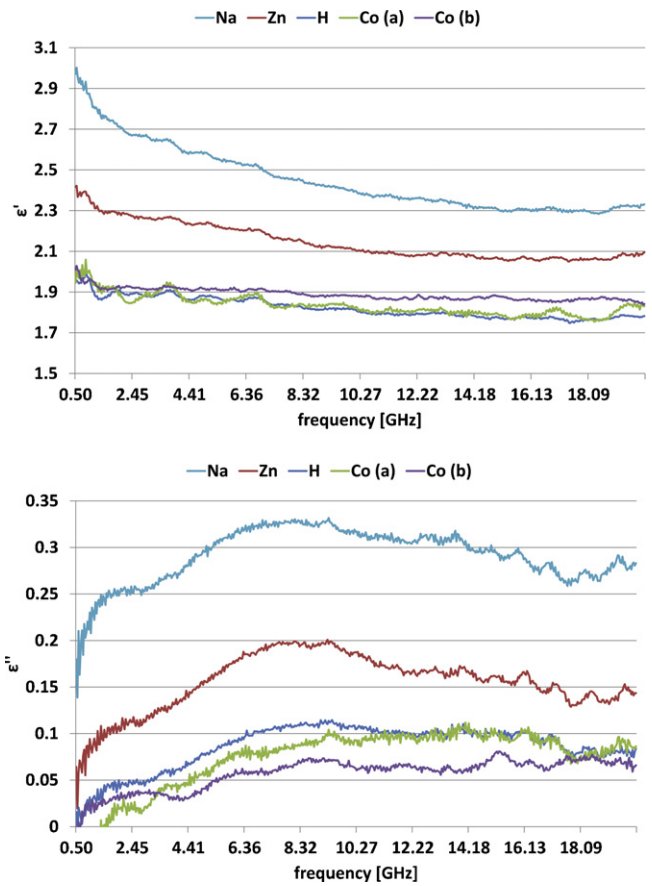

Fig. 3. Permittivity values (ε' and ε'') for partially dry FAU zeolites.

values weakness. This is caused by their poor ability to adsorb water (weak hydration compared to FAU zeolites) that turns difficult to compare them. Nevertheless, these weak values could be compared with those for Co(a).

An increase of the transition metal content in the zeolite structures produces a decrease in the complex dielectric permittivities values. A high metal content indicates a weak quantity of protons in the zeolites. During the ionic exchange process, the number of protons in the zeolite structure gets diminished [20]. The proton is monovalent and small. It is the most polarizable ion and it exists under the H_3O^+ that it forms with the oxygen atoms of the adsorbed water molecules in zeolites. So, it possesses a bigger mobility than the transition metal ions since it is able to move with the adsorbed water molecules across the cavities and channels, favoring the dielectric properties of the material. On the other hand, the transition metals are bivalent and they have a bigger size. That is why they find themselves strongly stuck in the zeolites framework due to steric effect. The observed MEL zeolites trend for dielectric permittivities values (Fig. 2) is in according to the transition metal ionic radius (Table 3).

Table 3
Ionic radius values for transition metal ions.

Transition metal ion	Ionic radius (nm)
H^+	0.0000015
Na^+	0.095
Fe^{3+}	0.064
Ni^{2+}	0.069
Mn^{3+}	0.046
Mn^{2+}	0.080
Zn^{2+}	0.074
Co^{2+}	0.078

For the partially dry FAU zeolites (10 wt% water) the trend is: Co(b) ≈ Co(a) ≈ H < Zn < Na and for the FAU that are saturated with water (33 wt% water), the trend is: Co(b) < Co(a) < Zn < H < Na as shown in Figs. 3 and 4, respectively.

The NaY dry zeolite possesses higher permittivities and its dielectric properties values differ from the others due to the strong decay of ε'' at low frequencies which represents an important ionic conductivity. This phenomenon can be observed in Fig. 5. The Na^+ cation moves easier in the zeolite framework, which allows a better interaction with the electrical field, and the observation of higher values of permittivities. This cation is monovalent, and it is not strongly attached to the oxygen atoms of the zeolite anionic framework in comparison to transition metals ions which are bivalents. The dielectric permittivities values are higher when the incorporated ions into zeolites are monovalent. The H-Y permittivities values are lower than those corresponding to Na-Y, because the proton is smaller than Na^+, and it is more polarizable. The proton exists under the H_3O^+ ion that could form with the oxygen atoms of the zeolite structure. In this case, it is not able to move because it is strongly attached to the oxygen atoms in the zeolites framework by their negative density charge [21]. It is only able to move when it is attached to the adsorbed water molecules in zeolites. The ionic ratio values are shown in Table 3.

3.2. Dielectric heating mechanisms in FAU and MEL zeolites

In order to understand the different mechanisms in the dielectric heating phenomenon, a modified Debye model was used for all zeolites [12,22,23]. From this model, it was possible to estimate the relaxation frequencies of each phenomenon by effecting a

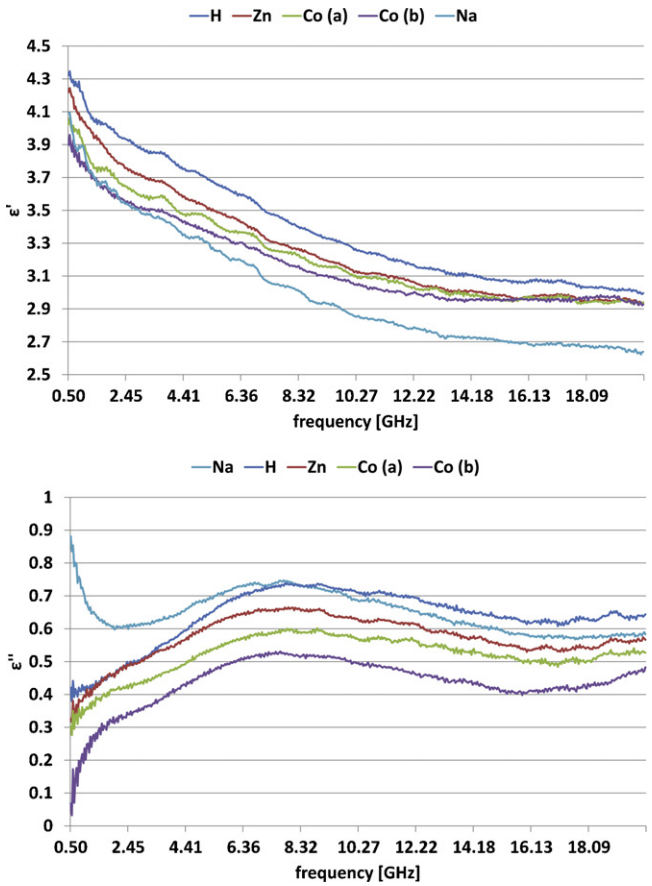

Fig. 4. Permittivity values (ε' and ε'') for saturated FAU zeolites.

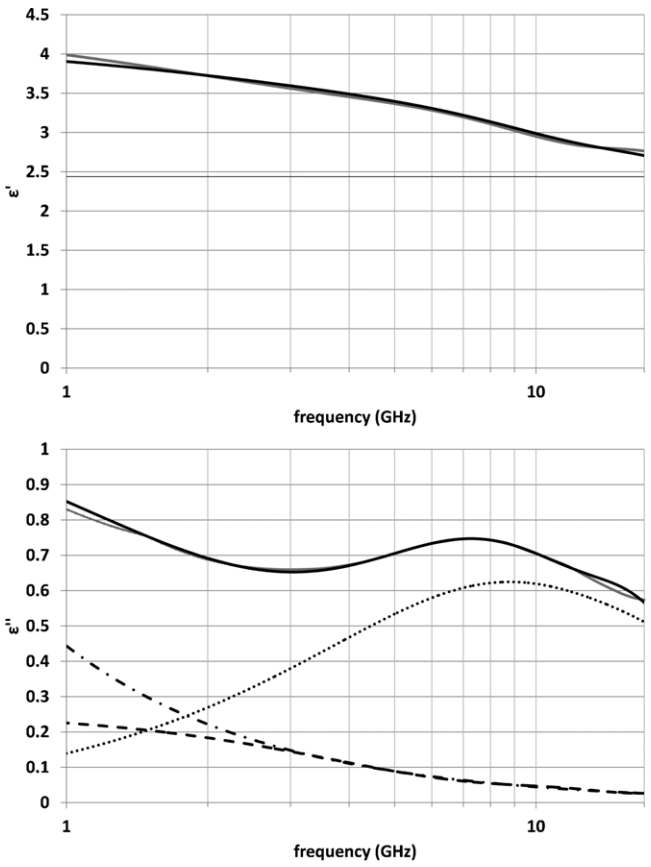

Fig. 6. Comparisons between the measured and calculated spectra for NaY zeolite 229 H_2O/u.c.: gray -, measured spectra; thick -, calculated spectra (sum curve); –, relaxation 1; ···, relaxation 2; -·-·-, conductivity contribution; -, ε_{inf}.

deconvolution of dielectric permittivity experimental curves. The model equations are shown below:

$$\begin{cases} \varepsilon'_r = \varepsilon_\infty + \dfrac{\varepsilon_{s1} - \varepsilon_\infty}{1+\omega^2\tau_1^2} + \dfrac{\varepsilon_{s2} - \varepsilon_\infty}{1+\omega^2\tau_2^2} \\ \varepsilon''_r = \dfrac{(\varepsilon_{s1} - \varepsilon_\infty)\omega\tau_1}{1+\omega^2\tau_1^2} + \dfrac{(\varepsilon_{s2} - \varepsilon_\infty)\omega\tau_2}{1+\omega^2\tau_2^2} + \dfrac{\sigma}{\omega\varepsilon_0} \end{cases} \quad \text{modified Debye model equations} \qquad (1)$$

where ω (rad s^{-1}) is the wave pulsation, ε_∞ is the permittivity at infinite frequency, ε_{si} are the static permittivities, τ_i ($1/2\pi f$) are the relaxation times and σ is the conductivity.

It was observed, for both type of zeolite FAU and MEL, a high relaxation frequency f_2 between 9 and 10 GHz owed to the rotational polarization of the adsorbed water molecules, and a low relaxation frequency f_1 between 0.7 and 1 GHz due to the interfacial polarization mechanism or Maxwell–Wagner's effect. The contribution of each dielectric phenomenon is shown in Fig. 6 for NaY zeolite. For all the zeolites, with the exception of the NaY, no ionic conductivity phenomenon was observed. The dielectric phenomena for this zeolite can be observed in Fig. 6.

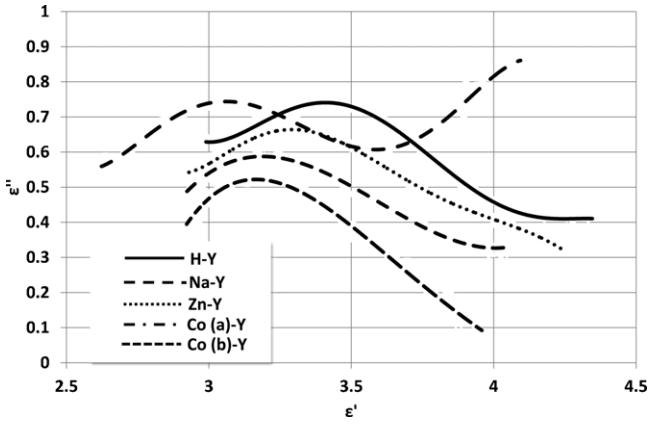

Fig. 5. Diagram of argand for saturated FAU zeolites (33 wt%), from 0.5 GHz to 20 GHz at room temperature (17 ± 2 °C).

3.3. Dielectric heating of zeolites under microwave irradiation

The absorption capacity of electromagnetic energy is higher for the FAU structure than MEL due to the presence of a higher number of cations per unit cell (See Tables 1 and 2). The monovalent cations move easier than the bivalent ones, because they are less attached to the negative zeolite framework, favoring the dielectric heating process. Also, the greater absorption capacity of electromagnetic energy for FAU is related to their bigger adsorption capacity of water molecules than MEL zeolites due to their different pore size and Si/Al ratio. In Table 4 the maximum values of temperature are given for each zeolite tested, measured in the center of the compacted and dehydrated zeolite bed. These zeolite compacted beds were heated under microwave irradiation until reaching thermal equilibrium between the absorbed power and thermal losses. At this stage, the measured temperature was constant.

In general, the bigger tan δ is, the greater the heating capacity of zeolites under microwave is. The FAU tend to heat more than MEL

Table 4
Maximum temperatures under microwave of zeolites FAU and MEL.

Zeolite	FAU (8 wt% water)				MEL (4 wt% water)		
Cation	Na^+	H^+	Zn^{2+}	Co^{2+}(a)	Co^{2+}(a)	Ni^{2+}	Mn^{2+}(a)
T max (°C)	75.86	80.80	52.50	31.65	45.80	41.10	55.20
tan δ 20 °C	0.078	0.101	0.013	0.005	NC[a]	0.023	0.028

[a] Non calculable.

due to the different water content for each structure. In spite of having effected the same treatment of dried or partial dehydration for every structure, before the measurements, it is not possible to obtain the same water content, since this one depends strictly on Si/Al ratio and on the pore size of every zeolite.

The observed heating capacity trend for FAU and MEL zeolites are in agreement with the tan δ values, which were estimated from the complex permittivity values measured at 2.45 GHz. The tan δ values, which were measured at room temperature, indicate the initial heating capacity for each zeolite. Thus, the bigger tan δ is, the greater the initial heating pulse of zeolites under microwave is. The final equilibrium temperature reached for each zeolite is partially linked to this initial heating pulse, it means, the tan δ values at room temperature.

3.4. Quantification of Lewis and Brönsted acid sites of zeolites

The number of Brönsted and Lewis acid sites were calculated from the maximum intensity of the absorption bands corresponding to the wavelengths of 1545 and 1450–1460 cm^{-1}, respectively and they were quantified using the extinction coefficients from literature [24], which are independent of the catalyst structure and from the acid force of the sites. In agreement with Emeis [24] the quantification of the Lewis and Brönsted acid sites was determined as μmol of pyridine adsorbed per mg of catalyst, for every zeolite. This determination was realized at three temperatures: 250, 350 and 400 °C in order to analyze the acid force of the acid sites in zeolites. The strong acid sites are those that retain the pyridine up to 400 °C. The sites of moderated acid force are given by the difference between the acid sites calculated at 400 °C and 350 °C and finally the weak acid sites are determined by the difference between the acid sites calculated at 350 and 250 °C.

The H-Y and H-ZSM-11 zeolites have the smallest L/B ratio due to the presence of protons in the structure. These zeolites were not submitted to the ionic exchange process for transition metal incorporation and the quantity of protons in the structure was not diminished [20]. On the other hand, the rest of the exchanged zeolites possess a significant increase of the L/B ratio.

The total number of acid sites is bigger for the FAU zeolites than the MEL zeolites, because the faujasites possess a low Si/Al ratio which means a more significant quantity of Al^{3+}cations and a greater deficiency of negative charge in the zeolite framework. A higher number of positive ions is necessary to neutralize the negative charge of the FAU zeolite structure. Besides, the FAU zeolites have a bigger pore size than MEL zeolites. For these reasons, FAU catalysts can incorporate a higher number of transition cations M^{2+} into their structures and they possess a greater quantity of acid sites than MEL zeolites. The different acid sites for every zeolite are shown in Table 5.

3.4.1. FTIR spectrum analysis for FAU and MEL zeolites

The FTIR spectrum analysis of pyridine adsorbed on FAU zeolites in the region between 1700 and 1350 cm^{-1} is shown in Fig. 7.

The zone between 1700 and 1350 cm^{-1} corresponds to the interaction of the pyridine molecules with Brönsted and Lewis acid sites [25,26]. The intensity of the Brönsted acid sites peaks at 1545 cm^{-1} decreases and confirms the protons consumption in zeolites after the ionic exchange process in agreement with Pierella et al. [6]. The signal at about 1635 cm^{-1} indicates the interaction with Brönsted acid sites (PyH^+).

Table 5
Lewis and Brönsted acid sites in FAU and MEL zeolites [μmol Py/mg cat.].

Zeolite structure	Cation	Brönsted sites	Lewis sites	Total	L/B
FAU (Y)	H	0.2862	0.0233	0.3095	0.0815
	Zn	0.1965	0.2668	0.4633	1.3576
	Co(a)	0.2041	0.2204	0.4245	1.0796
	Co(b)	0.1079	0.1447	0.2526	1.3405
MEL (ZSM-11)	H	0.0811	0.0086	0.0897	0.1056
	Co(a)	0.0596	0.1650	0.2246	2.7709
	Co(b)	0.0556	0.1547	0.2103	2.7806
	Co(c)	0.0454	0.0758	0.1212	1.6693
	Mn(a)	0.1173	0.0954	0.2127	0.8131
	Mn(b)	0.0624	0.1191	0.1815	1.9095
	Ni	0.0516	0.0617	0.1133	1.1966
	Fe	0.0794	0.0532	0.1326	0.6709

The bands observed at 1621–1615 cm^{-1} and 1454 cm^{-1} correspond to the adsorbed pyridine molecules on Lewis acid sites [25,26]. The sign at 1457 cm^{-1} observed in the parent zeolite corresponds to Lewis acid sites because of the Al^{3+} in the zeolite framework. The shift of this sign toward lower wave lengths (1454 cm^{-1}) reveals the superficial weakness of the acid sites [27,28]. The increase of Lewis acid sites after the incorporation of transition metal cations is probably produced by the formation of a new, strong electron-donor–acceptor (EDA) adduct of Pyridine-Lewis sites (L-Py).

The region between 1574 cm^{-1} and 1595 cm^{-1} corresponds to the physically adsorbed pyridine molecules linked to superficial hydroxyl groups by hydrogen bond [25,26]. The three previous interactions contribute to the band at 1489 cm^{-1} [25,26].

The FTIR spectrum analysis of pyridine adsorbed on MEL zeolites in the region between 1700 and 1400 cm^{-1} is shown in Fig. 8.

The 1452 cm^{-1} and 1612 cm^{-1} signals correspond to the pyridine interaction with Lewis acid sites [26]. The incorporation of transition metals in the zeolites produces an increase of Lewis acid sites. The bands at 1545 and 1635–1622 cm^{-1} demonstrate the pyridine interaction with Brönsted acid sites [29]. The zone at 1491 cm^{-1} represents the interaction of both previous effects [30,31]. H-ZSM-11 spectrum presents an important signal of Brönsted sites and some Lewis sites resulting from Al^{3+}. The incorporation of transition metal ions into zeolites diminishes the intensity of Brönsted acid sites bands. The formation of a new,

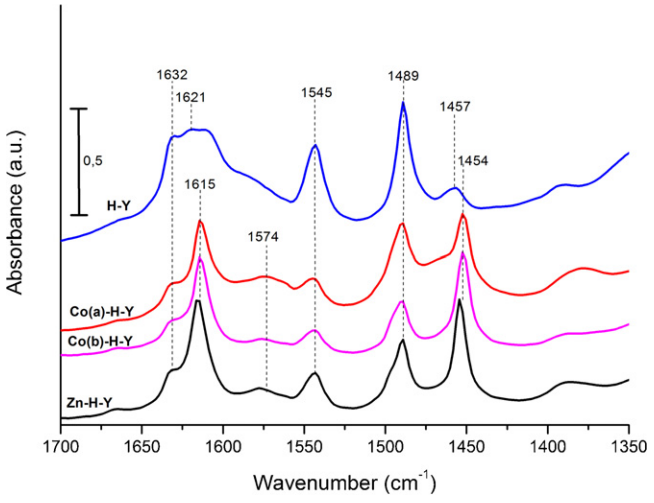

Fig. 7. FTIR spectra of pyridine adsorbed on FAU zeolites after evacuation at 400 °C and 10^{-4} Torr for 1 h, between 1700 and 1350 cm^{-1}.

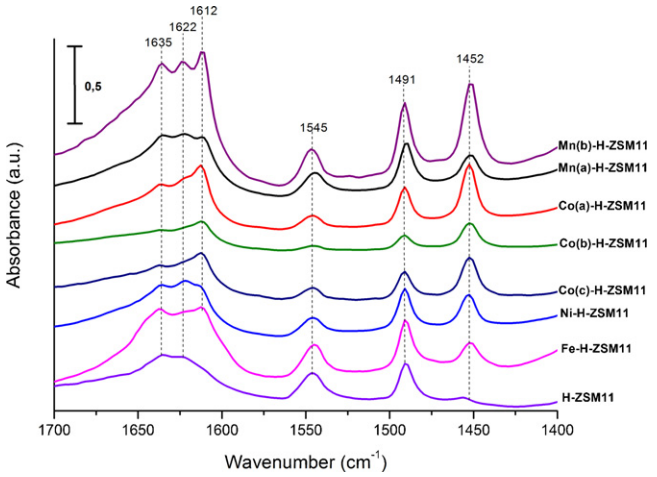

Fig. 8. FTIR spectra of pyridine adsorbed on MEL zeolites after evacuation at 400 °C and 10^{-4} Torr for 1 h, between 1700 and 1400 cm^{-1}.

strong electron-donor–acceptor (EDA) adduct of Pyridine-Lewis sites at 1452 cm^{-1} is clear, probably due to an interaction between a transition metal unoccupied molecular orbital and the pyridine, different from the well-known Lewis aluminum sites of the zeolites framework (1456 cm^{-1}).

3.5. Catalytic activity under microwave irradiation

In order to evaluate the performance of the zeolites doped with transition metals under microwave, the oxidation of styrene with hydrogen peroxide was carried out, for benzaldehyde production. The above mentioned reaction was repeated under identical conditions but using conventional and microwave heating in order to compare the two different heating forms. Others secondary products were found like styrene oxide, phenylacetaldehyde, benzoic acid and 1-phenylethane-1,2 diol in agreement with Maurya et al. [32]. Similar catalysts were studied by Saux and Pierella [33] in the same oxidation reaction under conventional heating, and they found that the reaction rate is first order with respect to styrene and oxidant concentration and the apparent activation energy is 14.54 kJ/mol. The selectivity toward benzaldehyde was found to be about 100% for all the cases. This fact indicates that this process allows to obtain the benzaldehyde without impurity traces and generation of pollutants.

The values of styrene conversion and selectivity toward benzaldehyde after 7 h of reaction are shown in Table 6.

The styrene conversion curves as a function of reaction time for MEL and FAU zeolites are shown in Figs. 9 and 10, respectively.

After 7 h of reaction, a maximum value of styrene conversion of 37% was obtained with Co(a)-H-ZSM-11 catalyst (Fig. 9 and Table 6). The value of selectivity toward benzaldehyde is about 100% for all the zeolites used in this study.

Table 6
Conversion and selectivity values under microwave heating.

Catalyst	Styrene conversion (% mol)	Selectivity (% mol)
Co(a)-H-ZSM-11	37.0%	90%
Co(b)-H-ZSM-11	23.0%	100%
Fe-H-ZSM-11	14.0%	100%
Mn(a)-H-ZSM-11	14.0%	100%
Co(a)-H-Y	10.0%	90%
H-ZSM-11	9.0%	100%
Ni-H-ZSM-11	8.7%	100%
Zn-H-Y	7.5%	100%
H-Y	7.3%	100%
Mn(b)-H-ZSM-11	4.5%	100%

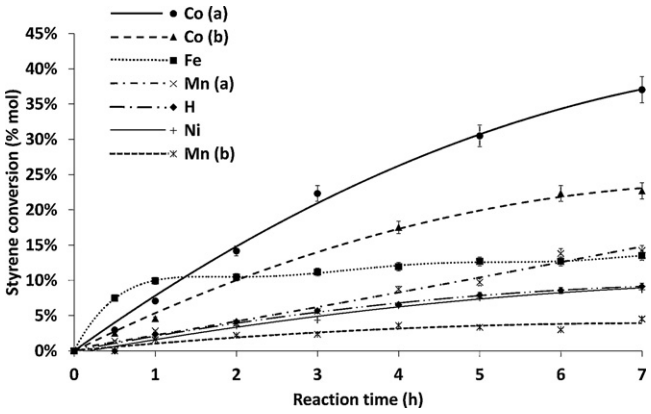

Fig. 9. Styrene conversion for MEL zeolites at 60 °C using 0.4 g of catalyst and acetonitrile as solvent at C_8H_8/H_2O_2 ratio = 0.9.

Cobalt catalysts are the most efficient for the reaction of partial styrene oxidation, for both FAU and MEL structures. The MEL zeolites doped with Co are more efficient than the zeolite Co(a)-H-Y. The Co-MEL zeolites have a bigger L/B ratio than Co-FAU zeolites, and they have a better catalytic activity than the FAU ones, in agreement with Pierella et al. [6]. The Lewis acid sites favor the catalytic behavior while Brönsted acid sites disfavor the benzaldehyde production and styrene conversion. Besides, the Lewis acid sites for FAU zeolites are located in the sites I (hexagonal prism) and the II (supercavity) [19]. Partly of the Lewis acid sites of FAU zeolites are hidden in the hexagonal prism and are inaccessible for the reaction reagents [34]. The lower activity for FAU zeolites is also due to the transition metal oxides that block the pore access.

For the MEL zeolites, the trend of the transition metals which is in agreement with the reaction efficiency for the styrene oxidation is: Co(a) > Co(b) > Fe > Mn(a) > H > Ni > Mn(b). For the FAU zeolites, the trend is: Co(a) > Zn > H.

The Fe catalyst presents a high activity in the styrene oxidation during the first hour of reaction, but it becomes constant the rest of the time, probably because of its rapid catalytic deactivation.

The generation of Lewis new acid sites by the incorporation of transition metals, increases the performance of the styrene oxidation reaction in agreement with Pierella et al. [6]. The zeolites doped with transition metals present a decrease of Brönsted acid sites and an increase of Lewis acid sites with respect to the pattern zeolite. Nevertheless the transition metal content introduced in the zeolite framework is not directly proportional to the quantity of generated Lewis sites. That is why the trend of the zeolites in the reaction performance of the styrene

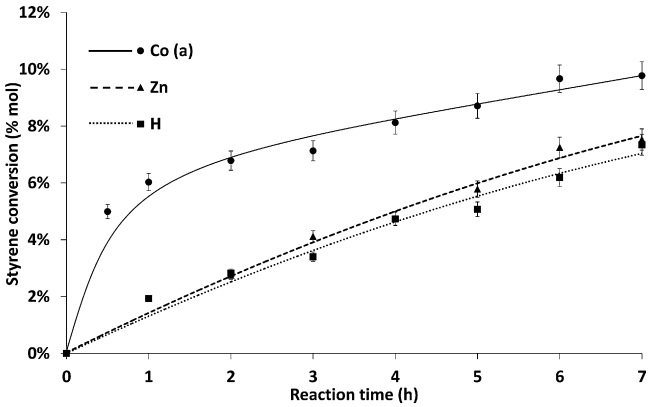

Fig. 10. Styrene conversion for FAU zeolites at 60 °C using 0.4 g of catalyst and acetonitrile as solvent at C_8H_8/H_2O_2 ratio = 0.9.

oxidation does not correspond to the transition metal content, but to the quantity of generated and accessible Lewis acid sites. The missing correlation could be explained by the formation of some species that do not contribute to the generation of Lewis acid sites. From Table 5, the following trend can be observed with respect to the quantity of Lewis acid sites for the ZSM-11 structure: Co(a) > Co(b) > Mn(b) > Mn(a) > Ni > Fe > H. For the FAU structure, the trend is: Zn > Co(a) > H. These trends are similar but do not exactly fit with those observed for the styrene conversion. In the MEL zeolites, Mn(b) is the third catalyst with respect to the quantity of Lewis acid sites; nevertheless it is the least efficient for this reaction. This fact is probably explained by the formation of oxide species as clusters that block the windows of the zeolites pores that prevent the diffusion of the reagents and products of reaction.

In addition, another important factor is the distribution homogeneity of transition metals inside the zeolites structure, which will depend on the ions diffusion across the zeolites channels during the ionic exchange process. This diffusion will be linked to the relation between the diameter of the transition metal ions and the pore diameter, according to the zeolite structure. The calcination process of zeolites at high temperature may facilitate the migration of metal transition from supercages to small cages due to the removal of coordinated water [35]. In this stage, the oxidation of the ions is produced. It may form an agglomeration of oxides and the access of reagents to the Lewis acid sites located in the small cages becomes difficult. In addition, there is also a certain quantity of transition metal located on the external surface of zeolites as the FTIR signal at 1574–1595 cm^{-1}. The quantity of agglomerated oxides in the entry of pores diminishes with the metal transition content incorporated into zeolites. That is why the Mn(a) presents a better activity than Mn(b). On the contrary, the Fe possesses less quantity of Lewis acid sites than Mn(a); nevertheless it has a better performance in the oxidation reaction. The Fe^{3+} ion is smaller than the Mn^{2+} and Mn^{3+} ions, thus it is distributed in a more homogeneous way in the zeolite framework. Its Lewis acid sites are more accessible than Mn sites, in spite of the existence of iron oxides clusters. The Mn ions are bigger than Fe ions and for that reason they possess a lower diffusion inside the zeolites channels causing heterogeneity in the distribution of Lewis acid sites. This fact restricts their complete utilization during the styrene oxidation reaction.

On the other hand, the cobalt ion has a bigger size than the Mn and Fe ions; nevertheless this ion is more difficultly oxidizable. Thus, the formation of Co oxides clusters turns out to be difficult. For the Co(a) and Co(b) catalysts, both trends coincide, which would indicate a maximum utilization of Lewis acid sites. The trend inversion for the Ni and pattern zeolite is not significant since the experimental relative error is 5%.

In FAU zeolites, the Zn catalyst has a higher quantity of Lewis acid sites than Co(a). Unlike the observed behavior for MEL zeolites, the quantity of transition metal incorporated into zeolites is in agreement with the quantity of generated Lewis acid sites. Nevertheless Co(a) presents a better performance in the styrene oxidation reaction. Since the Zn content is superior to that of Co inside the zeolites, the quantity of Zn oxides clusters is probably more significant than in the Co catalyst. A more important diffusion difficulty of reagents and products is observed for Zn. That is why it presents a lower performance in the styrene oxidation reaction.

3.6. Microwave irradiation VS conventional heating

The Co(b) and Mn(b) catalysts of the MEL structure were used in order to compare the difference between microwave and conventional heating. The curves of styrene conversion as a function of reaction time, for both sort of heating, are shown in Fig. 11.

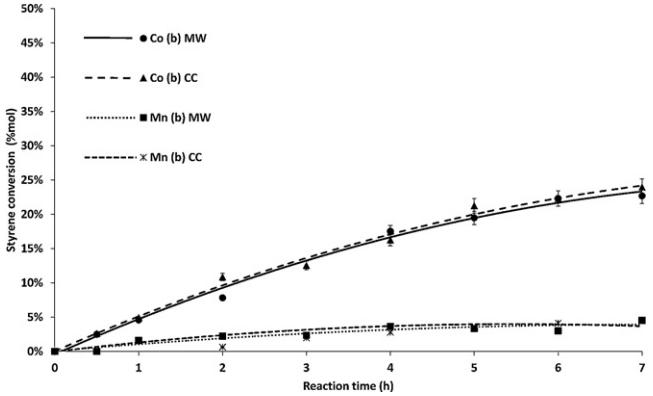

Fig. 11. Styrene conversion for FAU and MEL zeolites under microwave irradiation and conventional heating at 60 °C using 0.4 g of catalyst and acetonitrile as solvent at C_8H_8/H_2O_2 ratio = 0.9.

The styrene conversion for Co(b) is 23% whereas for Mn(b) is 4.5%. The selectivity toward benzaldehyde was 100% for all the cases.

No difference in terms of styrene conversion and benzaldehyde production was observed between the two heating form used. Any particular interaction between microwaves and zeolites particles was observed. In order to achieve a better catalytic performance under microwave irradiation, it is necessary to heat the solid catalyst moreover than the solvent of the reaction system. In these experiences, the catalyst was in suspension in the shape of finely divided powder. The interaction catalyst–electromagnetic energy is not significant and the reaction system behaves in the same way as under conventional heating.

In order to turn the dielectric heating of zeolites as significant as the solvent one, it is probably necessary to use the zeolite catalysts under a compact structure. The catalytic activity for the Co zeolite is superior to the Mn zeolite activity for the styrene oxidation in agreement with Pierella et al. [6] in terms of styrene conversion and benzaldehyde production.

4. Conclusions

MEL and FAU zeolites doped with transition metals were prepared. The dielectric properties of these solids showed that the faujasites possess higher dielectric properties values than ZSM-11, especially thanks to a higher possibility of hydration; fact which would allow a better performance under microwave heating. The nature of the transition metal and the quantity of ions per unit cell are two parameters that influence the dielectric properties values. The dielectric properties were higher for monovalent cation than bivalent, due to higher ion mobility across the zeolites structure. The complex dielectric permittivities values diminished with the increase of the transition metal content. An augmentation of the number of transition metals per unit cell implies an increase of ion density that obstructs the mobility of the same ones. Only the NaY zeolite presented ionic conductivity at low frequency, due to the mobility of the Na^+ ions at high water content. The response of this solid to the microwave irradiation agrees with the measured dielectric properties. With the use of a modified Debye model, the responsible mechanisms for the zeolite dielectric heating were determined. The existence of the ionic conductivity phenomenon in the hydrated NaY zeolite was verified. For all the zeolites, the phenomenon of interfacial polarization Maxwell–Wagner with relaxation frequency of 1 GHz and the phenomenon of rotational polarization of adsorbed water molecules with relaxation frequency of 9 GHz were verified.

The transition metal content was estimated for every zeolite by ICP. By performing a FTIR study of pyridine adsorption in zeolites the quantity of Lewis and Brönsted acid sites was estimated.

The transition metal incorporation into FAU and MEL zeolites causes a Lewis acid sites increase and a Brönsted acid sites decrease. The global quantity of acid sites is increased by transition metal incorporation.

The number of incorporated cations in the zeolite structures is related to the number of acid sites and in consequence to the catalytic activity. It was found that FAU zeolites possess a greater quantity of acid sites than MEL zeolites. The higher available Lewis acid sites are, the greater the styrene conversion is. FAU zeolites reaction activity is lower than MEL zeolites spite of having the higher acid sites content. This is because the FAU total quantity of Lewis acid sites is not usable.

Styrene oxidation reactions were carried out under microwave and conventional heating. The results show a strong influence of the nature of the transition metal incorporated in zeolites and of the structure type. The more effective catalyst was found to be the MEL zeolites doped with cobalt. The quantity of Lewis acid sites is higher in FAU zeolites than in MEL zeolites. Nevertheless, the MEL structure is more efficient in the styrene oxidation reaction than FAU zeolites because of its lower transition metal content, which implies a diminution of the formation of transition metal oxides clusters in the channels of zeolites. These clusters are believed to be responsible for the diffusion obstruction of reaction reagents and products. Besides, partly of the new generated Lewis acid sites for FAU zeolites are inaccessible for the reaction reagents since they are located in the hexagonal prism of the zeolite structure.

No difference between microwave and conventional heating was observed with regard to the styrene conversion and selectivity toward benzaldehyde. In order to optimize the benzaldehyde production process under microwave irradiation it is necessary to re-design the catalysts toward a compact form. Thus, the catalyst–electromagnetic energy interaction would become significant and it would overcome the conventional heating governed by the slow convective heating phenomenon.

Acknowledgements

This project was partially supported by: Foncyt PICT 2007-00303, Mincyt-Córdoba PID 000121 and PID UTN 25/E129. We thank CONICET-Argentina.

References

[1] A. Stankiewicz, Chem. Eng. Process. 42 (2003) 137–144.
[2] P.T. Anastas, M.M. Kirchhoff, T.C. Williamson, Appl. Catal. A: Gen. 221 (2001) 3–13.
[3] J. Galownia, J. Martín, M.E. Davis, Microporous Mesoporous Mater. 92 (2006) 61–63.
[4] M.A. Zanjanchi, S. Sohrabnezhad, Sens. Actuators B 105 (2005) 502–507.
[5] M. Tsapatsis, M. Lovallo, T. Okubo, M.E. Davis, M. Sadakata, Chem. Mater. 7 (1995) 1734–1741.
[6] L.B. Pierella, C. Saux, S. Caglieri, H. Bertorello, P.G. Bercoff, Appl. Catal. A: Gen. 347 (2008) 55–61.
[7] S. Das, A. Mukhopadhyay, S. Datta, D. Basu, Bull. Mater. Sci. 31 (2008) 943–956.
[8] E. Thostenson, T. Chou, Compos. Part A: Appl. Sci. 30 (1999) 1055–1071.
[9] G. Roussy, A. Pearce, Foundations and Industrial Applications of Microwaves and Radio Frequency Fields Physical and Chemical Processes, first ed., Wiley, New York, 1995.
[10] R. Pan, Y. Wu, Q. Wang, Y. Hong, Chem. Eng. J. 153 (2009) 206–210.
[11] P. Patil, V. Gnaneswar Gude, S. Pinappu, S. Deng, Chem. Eng. J. 168 (2011) 1296–1300.
[12] B. Legras, I. Polaert, L. Estel, M. Thomas, J. Phys. Chem. C 115 (7) (2011) 3090–3098.
[13] S. Sithambaram, E.K. Nyutu, S.L. Suib, Appl. Catal. A: Gen. 348 (2008) 214–220.
[14] N. Lingaiah, K.M. Reddy, N.S. Babu, K.N. Rao, I. Suryanarayana, P.S.S. Prasad, Catal. Commun. 7 (2006) 245–250.
[15] V.N. Shetti, J. Kim, R. Srivastava, M. Choi, R. Ryoo, J. Catal. 254 (2008) 296–303.
[16] I. Polaert, L. Estel, R. Huyghe, M. Thomas, Chem. Eng. J. 162 (2010) 941–948.
[17] S. Koichi, N. Yoichi, M. Nobuyuki, I. Motoyasu, S. Hiromichi, Microporous Mater. 59 (2003) 133–146.
[18] J. Dedecek, D. Kaucky, B. Wichterlova, Microporous Mesoporous Mater. 35/36 (2000) 483–494.
[19] T. Frising, P. Leflaive, Microporous Mesoporous Mater. 114 (2008) 27–63.
[20] M. Mhamdi, S. Khaddar-Zine, A. Ghorbel, Appl. Catal. A: Gen. 337 (2008) 39–47.
[21] A. Abdoulaye, S.S. Soulaymanl, G. Chabanis, J.C. Giuntini, J.V. Zanchetta, Microporous Mater. 8 (1997) 63–68.
[22] J. Macutkevic, J. Banys, A. Matulis, Nonlinear Anal. 9 (2004) 75–88.
[23] U.J. Kaatze, J. Solution Chem. 26 (1997) 1049–1112.
[24] C.A. Emeis, J. Catal. 141 (1993) 347–354.
[25] M.R. Basila, T.R. Kantner, K.H. Rhee, J. Phys. Chem. 68 (1964) 3197–3207.
[26] F. Thibault-Starzyk, B. Gil, S. Aiello, T. Chevreau, J. Gilson, Microporous Mesoporous Mater. 67 (2004) 107–112.
[27] M. Schwidder, M. Santhosh Kumar, U. Bentrup, J. Pérez-Ramírez, A. Brückner, W. Grünert, Microporous Mesoporous Mater. 111 (2008) 124–133.
[28] M. Mohamed, F. Zidan, M. Thabet, Microporous Mesoporous Mater. 108 (2008) 193–203.
[29] G. Busca, Phys. Chem. Chem. Phys. 1 (1999) 723–736.
[30] K.H. Rhee, V. Udaya, S. Rao, J.M. Stencel, G.A. Melson, J.E. Crawford, Zeolites 3 (1983) 337–343.
[31] R. Borade, A. Sayari, A. Adnot, S. Kaliaguine, J. Phys. Chem. 94 (1990) 5989–5994.
[32] M.R. Maurya, A.K. Chandrakar, S. Chand, J. Mol. Catal. A: Chem. 274 (2007) 192–201.
[33] C. Saux, L.B. Pierella, Appl. Catal. A: Gen. 400 (2011) 117–121.
[34] K. Gora-Marek, Vib. Spectrosc. 52 (2010) 31–38.
[35] S. Hu, D. Liu, C. Wang, Y. Chen, Z. Guo, A. Borgna, Y. Yang, Appl. Catal. A: Gen. 386 (2010) 74–82.